8

Integrated Design of IIR Variable Fractional Delay Digital Filters with Variable and Fixed Denominators

Hon Keung Kwan and Aimin Jiang
Department of Electrical and Computer Engineering
University of Windsor, Windsor, ON N9B 3P4
Canada

1. Introduction

In this chapter, the following abbreviations are used: Variable-denominator IIR VFD filters as VdIIR VFD filters. Fixed-denominator IIR VFD filters as FdIIR VFD filters. Allpass VFD filters as AP VFD filters. FIR VFD filters the same as FIR VFD filters. Symbol t is used to represent fractional delay (instead of the symbol d normally used to denote the operation of differentiation). Five frequently referenced design methods are abbreviated for ease of reference in Sections 5-8 as: (Zhao & Kwan, 2007) as (ZK); (Kwan & Jiang, 2009a) as (KJ); (Tsui et al., 2007) as (TCK); (Lee et al., 2008) as (LCR); and (Lu & Deng, 1999) as (LD).

Variable fractional delay (VFD) digital filters have various applications in signal processing and communications (Laakso et al., 1996). So far, finite impulse response (FIR) VFD digital filters have been studied and a number of design methods (Deng, 2001; Deng & Lian, 2006; Kwan & Jiang, 2009a, 2009b; Lu & Deng, 1999; Tseng, 2002a; Zhao & Yu, 2006) have been advanced. Since the frequency response of an FIR VFD filter is a linear function of its polynomial coefficients, an optimal design can be obtained by numerical procedures (Kwan & Jiang, 2009a, 2009b; Tseng, 2002a; Zhao & Yu, 2006) or in closed forms (Deng, 2001; Deng & Lian, 2006; Lu & Deng, 1999). In contrast to FIR VFD filter design, allpass (AP) VFD filter design faces additional challenges due to the existence of a denominator. Since allpass VFD filters have fullband unity magnitude responses, the problem of designing an allpass VFD filter is to minimize the approximation error of phase or group delay response between an allpass VFD filter to be designed and the ideal one. A number of algorithms (Lee, et al., 2008; Tseng, 2002a, 2002b) have been proposed based on this strategy. Another property of allpass VFD filters which has been exploited in (Kwan & Jiang, 2009a; Deng, 2006) is the mirror symmetric relation between the numerator and the denominator. Such algorithms (Kwan & Jiang, 2009a; Deng, 2006) minimize the approximation error in terms of frequency responses of the denominator. The resulting problem is nonconvex, which is either simplified and solved (Kwan & Jiang, 2009a) as a quadratic programming (QP) problem with positive-realness-based stability constraints, or solved (Deng, 2006) in closed-form.

Results obtained in (Kwan & Jiang, 2009a, 2009b; 2007) indicate that general infinite impulse response (IIR) digital filters exhibit lower mean group delay (compared to allpass digital filters) and wider band characteristics (compared to allpass and FIR digital filters) in VFD filter design. In general, general IIR VFD filter design methods (Kwan et al., 2006; Kwan & Jiang, 2007, 2009a, 2009b; Tsui et al., 2007; Zhao & Kwan, 2005, 2007; Zhao et al., 2006) can be classified as two-stage approach and semi-integrated approach. Under the two-stage approach (Kwan et al., 2006; Kwan & Jiang, 2007, 2009a, 2009b; Zhao & Kwan, 2005, 2007; Zhao et al., 2006), a set of stable IIR digital filters with sampled fractional delays (FDs) are designed first, and then the polynomial coefficients are determined by fitting the obtained IIR FD filter coefficients in the least-squares (LS) sense. Under the semi-integrated approach (Tsui et al., 2007), direct optimization is carried out on the polynomial coefficients of each filter coefficient of the numerator. In (Kwan et al., 2006; Kwan & Jiang, 2007; Zhao & Kwan, 2005, 2007; Zhao et al., 2006), both the numerator and denominator coefficients are variable. In (Kwan & Jiang, 2009a, 2009b; Tsui et al., 2007), only the numerator coefficients are variable. In (Kwan & Jiang, 2007), both variable and fixed denominators are considered.

In this chapter, sequential and gradient-based methods are applied to design IIR VFD filters with variable and fixed denominators, but unlike (Kwan & Jiang, 2007), these methods are integrated design methods. Second-order cone programming (SOCP) is used to formulate the problem in the sequential design method, and in the initial design of the gradient-based design method. An advantage of using the SOCP formulation of the problem is that both linear and (convex) quadratic constraints can be readily incorporated. On the other hand, unlike the design algorithm of (Tsui et al., 2007), which models the denominator and optimizes the numerator separately, the proposed methods optimize them simultaneously during the design procedures. As described in this chapter, the sequential and especially the gradient-based design methods could achieve some improved results as compared to (a) our previous designs presented in (Zhao & Kwan, 2007) for variable-denominator IIR VFD filters, in (Kwan & Jiang, 2009a) and (Tsui et al., 2007) for fixed-denominator IIR VFD filters, and in (Kwan & Jiang, 2009a) for allpass and FIR VFD filters; and (b) the allpass (Lee et al., 2008) and the FIR (Lu & Deng, 1999) VFD filters of other researchers. A preliminary version of the sequential design method can be found in (Jiang & Kwan, 2009b). The chapter is organized as follows: In Section 2, the weighted least-squares (WLS) design problem is formulated. A sequential design method is introduced in Section 3. Then, a gradient-based design method is introduced in Section 4. Four sets of filter examples are presented in Section 5 and their design performances using the proposed and a number of other methods are analyzed in Section 6. Section 7 gives a summary of the chapter. Finally, conclusions are made in Section 8.

2. Problem formulation

Let the ideal frequency response of a VFD digital filter be defined as

$$H_d(\omega, t) = e^{-j(D+t)\omega}, \quad \omega \in [0, \alpha\pi] \tag{1}$$

where $0 < \alpha < 1$, D denotes a mean group delay, and t denotes a variable fractional delay within the range of [−0.5, 0.5]. The transfer function of an IIR VFD filter can be expressed as

$$H(z,t)=\frac{P(z,t)}{Q(z,t)}=\frac{\sum_{n=0}^{N}p_n(t)z^{-n}}{1+\sum_{m=1}^{M}q_m(t)z^{-m}}=\frac{\boldsymbol{\varphi}_1^T(z)\boldsymbol{p}(t)}{1+\boldsymbol{\varphi}_2^T(z)\boldsymbol{q}(t)} \tag{2}$$

where

$$\boldsymbol{\varphi}_1(z)=\begin{bmatrix}1 & z^{-1} & \cdots & z^{-N}\end{bmatrix}^T \tag{3}$$

$$\boldsymbol{\varphi}_2(z)=\begin{bmatrix}z^{-1} & z^{-2} & \cdots & z^{-M}\end{bmatrix}^T \tag{4}$$

$$\boldsymbol{p}(t)=\begin{bmatrix}p_0(t) & p_1(t) & \cdots & p_N(t)\end{bmatrix}^T \tag{5}$$

$$\boldsymbol{q}(t)=\begin{bmatrix}q_1(t) & q_2(t) & \cdots & q_M(t)\end{bmatrix}^T \tag{6}$$

In (2)-(6), the superscript T denotes the transposition of a vector (or matrix). Each of the numerator coefficients $p_n(t)$ for n = 0, 1, …, N (or the denominator coefficients $q_m(t)$ for m = 1, 2, …, M) can be expressed as an order K_1 (or K_2) polynomial of the fractional delay t as

$$p_n(t)=\sum_{k=0}^{K_1}a_{n,k}t^k=\boldsymbol{a}_n^T\boldsymbol{v}_1(t) \tag{7}$$

$$q_m(t)=\sum_{k=0}^{K_2}b_{m,k}t^k=\boldsymbol{b}_m^T\boldsymbol{v}_2(t) \tag{8}$$

where

$$\boldsymbol{v}_1(t)=\begin{bmatrix}1 & t & \cdots & t^{K_1}\end{bmatrix}^T \tag{9}$$

$$\boldsymbol{v}_2(t)=\begin{bmatrix}1 & t & \cdots & t^{K_2}\end{bmatrix}^T \tag{10}$$

$$\boldsymbol{a}_n=\begin{bmatrix}a_{n,0} & a_{n,1} & \cdots & a_{n,K_1}\end{bmatrix}^T \tag{11}$$

$$\boldsymbol{b}_m = \begin{bmatrix} b_{m,0} & b_{m,1} & \cdots & b_{m,K_2} \end{bmatrix}^T \tag{12}$$

All the polynomial coefficients $a_{n,k}$ and $b_{m,k}$ are assumed to be real values. By stacking all $\boldsymbol{a}_n$ for $n = 0$ to N together, the numerator coefficient vector $\boldsymbol{a}$ can be defined as

$$\boldsymbol{a} = \begin{bmatrix} \boldsymbol{a}_0^T & \boldsymbol{a}_1^T & \cdots & \boldsymbol{a}_N^T \end{bmatrix}^T \tag{13}$$

Similarly, the denominator coefficient vector $\boldsymbol{b}$ can be defined as

$$\boldsymbol{b} = \begin{bmatrix} \boldsymbol{b}_1^T & \boldsymbol{b}_2^T & \cdots & \boldsymbol{b}_M^T \end{bmatrix}^T \tag{14}$$

Then, $P(z,t)$ and $Q(z,t)$ in (2) can be written as

$$P(z,t) = \boldsymbol{a}^T \boldsymbol{u}_1(z,t) \tag{15}$$

$$Q(z,t) = 1 + \boldsymbol{b}^T \boldsymbol{u}_2(z,t) \tag{16}$$

where

$$\boldsymbol{u}_1(z,t) = \begin{bmatrix} \boldsymbol{v}_1^T(t) & z^{-1}\boldsymbol{v}_1^T(t) & \cdots & z^{-N}\boldsymbol{v}_1^T(t) \end{bmatrix}^T \tag{17}$$

$$\boldsymbol{u}_2(z,t) = \begin{bmatrix} z^{-1}\boldsymbol{v}_2^T(t) & z^{-2}\boldsymbol{v}_2^T(t) & \cdots & z^{-M}\boldsymbol{v}_2^T(t) \end{bmatrix}^T \tag{18}$$

Given a nonnegative weighting function $W(\omega,t)$, the WLS design problem can be expressed as

$$\min_{\boldsymbol{x}} \quad J(\boldsymbol{x}) = \int_0^{\alpha\pi} \int_{-0.5}^{0.5} W(\omega,t) \left| e(\omega,t) \right|^2 dt d\omega \tag{19}$$

where $\boldsymbol{x} = [\boldsymbol{a}^T, \boldsymbol{b}^T]^T$, and the complex approximation error $e(\omega,t)$ is defined as

$$e(\omega,t) = H(e^{j\omega},t) - H_d(\omega,t) \tag{20}$$

For the general IIR VFD filter design problem expressed in (19), there is an implicit stability requirement on the denominator $Q(z,t)$, that is, all the roots of $Q(z,t)$ for $\forall t \in [-0.5, 0.5]$ should lie inside the unit circle on the z-plane. The derivations shown under Sections 2-4 are formulated for VdIIR VFD filters which are applicable to FdIIR VFD filters by setting $K_2 = 0$. For $K_2 = 0$, $q_m(t) = q_m$ for $m = 1$ to M; hence, $\boldsymbol{q}(t) = \boldsymbol{q} = [q_1\ q_2\ \ldots\ q_M]^T$ and $Q(z,t) = Q(z)$.

3. Sequential design of IIR VFD digital filters

The nonlinear nature of the general problem defined by (19)-(20) can be simplified using the Levy's method (Levy, 1959), solved iteratively using Sanathanan and Koerner algorithm (Sanathanan & Koerner, 1963), and formulated as an iterative design problem for stable IIR digital filters by (Lu et al., 1998). In this section, the sequential design procedure for IIR VFD filters developed from (Lu et al., 1998) will be described first. Then, linear inequality constraints are introduced to guarantee the stability of a designed IIR VFD filter.

3.1 Sequential design procedure

The sequential design procedure starts from a specified initial point $\boldsymbol{x}^{(0)}$. At the lth iteration (l = 1, 2, …), the integrand of the cost function in (19) is reformulated as

$$\begin{aligned} & W^{(l-1)}(\omega,t)\left|P^{(l)}(e^{j\omega},t)-H_d(\omega,t)Q^{(l)}(e^{j\omega},t)\right|^2 \\ &= W^{(l-1)}(\omega,t)\left|\boldsymbol{x}^{(l)T}\boldsymbol{u}(\omega,t)-e^{-j(D+t)\omega}\right|^2 \\ &= W^{(l-1)}(\omega,t)\boldsymbol{x}^{(l)T}\,\mathrm{Re}\left\{\boldsymbol{U}(\omega,t)\right\}\boldsymbol{x}^{(l)} \\ &\quad -2W^{(l-1)}(\omega,t)\boldsymbol{x}^{(l)T}\,\mathrm{Re}\left\{\boldsymbol{u}(\omega,t)e^{j(D+t)\omega}\right\} \\ &\quad +W^{(l-1)}(\omega,t) \end{aligned} \tag{21}$$

where

$$W^{(l-1)}(\omega,t)=\frac{W(\omega,t)}{\left|Q^{(l-1)}(e^{j\omega},t)\right|^2} \tag{22}$$

$$\boldsymbol{u}(\omega,t)=\begin{bmatrix}\boldsymbol{u}_1(e^{j\omega},t)\\ -e^{-j(D+t)\omega}\boldsymbol{u}_2(e^{j\omega},t)\end{bmatrix} \tag{23}$$

$$\begin{aligned} & \boldsymbol{U}(\omega,t) \\ &= \boldsymbol{u}(\omega,t)\boldsymbol{u}^H(\omega,t) \\ &= \begin{bmatrix}\boldsymbol{u}_1(e^{j\omega},t)\boldsymbol{u}_1^H(e^{j\omega},t) & -e^{j(D+t)\omega}\boldsymbol{u}_1(e^{j\omega},t)\boldsymbol{u}_2^H(e^{j\omega},t)\\ -e^{-j(D+t)\omega}\boldsymbol{u}_2(e^{j\omega},t)\boldsymbol{u}_1^H(e^{j\omega},t) & \boldsymbol{u}_2(e^{j\omega},t)\boldsymbol{u}_2^H(e^{j\omega},t)\end{bmatrix} \end{aligned} \tag{24}$$

In (21), Re{·} denotes the real part of a complex variable. In (24), the superscript H represents the conjugate transpose of a complex-valued vector or matrix. Using (21), the cost function of (19) can be expressed in the following quadratic form

$$J^{(l)}(\boldsymbol{x}^{(l)})=\boldsymbol{x}^{(l)T}\boldsymbol{G}^{(l-1)}\boldsymbol{x}^{(l)}-2\boldsymbol{x}^{(l)T}\boldsymbol{g}^{(l-1)}+c^{(l-1)} \tag{25}$$

where

$$\boldsymbol{G}^{(l-1)} = \int_0^{\alpha\pi} \int_{-0.5}^{0.5} W^{(l-1)}(\omega,t)\,\mathrm{Re}\{\boldsymbol{U}(\omega,t)\}\,dtd\omega \tag{26}$$

$$\boldsymbol{g}^{(l-1)} = \int_0^{\alpha\pi} \int_{-0.5}^{0.5} W^{(l-1)}(\omega,t)\,\mathrm{Re}\{\boldsymbol{u}(\omega,t)e^{j(D+t)\omega}\}\,dtd\omega \tag{27}$$

$$c^{(l-1)} = \int_0^{\alpha\pi} \int_{-0.5}^{0.5} W^{(l-1)}(\omega,t)dtd\omega \tag{28}$$

Note that the matrix $\boldsymbol{G}^{(l-1)}$ is symmetric and positive semidefinite (PSD). Therefore, only the upper (or lower) triangular part of $\boldsymbol{G}^{(l-1)}$ needs to be computed. In practice, the integrals in (26)-(28) can be replaced by finite summations of grid points taken from $[0,\ \alpha\pi] \times [-0.5, 0.5]$. In practice, minimization of (25) is a straight-forward task. However, if linear or nonlinear constraints (such as the linear stability constraints (34) or (35) introduced later in Section 3.2) are required to be incorporated, (25) can be reformulated as (29) by introducing an auxiliary variable $\varepsilon^{(l)}$. Consequently, at the lth iteration, the WLS design problem can be cast as the following SOCP problem

$$\min\ \varepsilon^{(l)} \tag{29}$$

$$\text{s.t. } \left\|\bar{\boldsymbol{G}}^{(l-1)}\boldsymbol{x}^{(l)}\right\|^2 \le 2\boldsymbol{x}^{(l)T}\boldsymbol{g}^{(l-1)} + \varepsilon^{(l)} \tag{29a}$$

where $\bar{\boldsymbol{G}}^{(l-1)} = [\boldsymbol{G}^{(l-1)}]^{1/2}$, and $\|.\|$ denotes the Euclidean norm of a vector. In (29), the decision variables are $\boldsymbol{x}^{(l)}$ and $\varepsilon^{(l)}$. The constraint (29a) is a hyperbolic constraint, which can be further transformed into a second-order cone (SOC) constraint.

To guarantee the stability of a design obtained by (29), either the stability constraints (34) or (35) are to be incorporated into (29). Also, to improve the numerical robustness of the sequential design procedure, the filter coefficients $\boldsymbol{x}^{(l)}$ are updated using the iteration scheme (Jiang & Kwan, 2009a; Lu et al., 1998; Lu, 1999; Tsang, 2004; Tsang & Lee, 2002) as

$$\boldsymbol{x}^{(l)} = \lambda\Psi(\boldsymbol{x}^{(l-1)}) + (1-\lambda)\boldsymbol{x}^{(l-1)} \tag{30}$$

where $0 < \lambda < 1$ is a relaxation constant, and Ψ represents the mathematical operation of mapping a $\boldsymbol{x}^{(l-1)}$ to a solution $\boldsymbol{x}^{(l)}$ by (29). Our design experience indicates that generally λ can be chosen within the range [0.1, 0.5]. A larger λ could cause numerical instability. Stability guarantee and robustness improvement serve different purposes and do not affect each other.

The sequential design procedure continues until the following condition is satisfied

$$\frac{J(\boldsymbol{x}^{(l-1)}) - J(\boldsymbol{x}^{(l)})}{J(\boldsymbol{x}^{(l-1)})} \le \mu \tag{31}$$

where μ is a specified positive small tolerance and $J(\boldsymbol{x})$ is the cost function defined in (19). The stopping criterion (31) means that the sequential design procedure is to be terminated as the WLS error cannot be further reduced in a meaningful manner. It should be emphasized that if $[J(\boldsymbol{x}^{(l-1)})-J(\boldsymbol{x}^{(l)})]/J(\boldsymbol{x}^{(l-1)}) < 0$, we have $J(\boldsymbol{x}^{(l-1)}) < J(\boldsymbol{x}^{(l)})$, which means the performance of the current design is worse than that of the previous design, the filter coefficients obtained at the previous iteration through (30) should be restored and adopted as the final design.

3.2 Stability consideration

The IIR VFD filter designed by the sequential design procedure presented in Section 3.1 cannot definitely guarantee the stability of obtained IIR VFD filters. Therefore, stability constraints have to be incorporated. For ease of explanation, a stability constraint based on the positive realness is first introduced for designing IIR VFD filters with the fixed denominator. Then, the stability constraint can be readily extended to the case of designing IIR VFD filters with the variable denominator.

A sufficient condition for the stability of designed IIR digital filters has been introduced in (Dumitrescu & Niemistö, 2004), which is stated as: If $Q^{(l-1)}(z)$ is a Schur polynomial, i.e., all the roots of $Q^{(l-1)}(z)$ lie inside the unit circle, and the transfer function $R^{(l)}(z) = Q^{(l)}(z)/Q^{(l-1)}(z)$ is strictly positive real (SPR), i.e.,

$$\mathrm{Re}\left\{R^{(l)}(e^{j\omega})\right\} > 0, \quad \forall\, \omega \in [0, \pi] \tag{32}$$

then all the convex combination of $Q^{(l-1)}(z)$ and $Q^{(l)}(z)$, i.e., $Q_\gamma^{(l)}(z) = (1-\gamma)Q^{(l-1)}(z)+\gamma Q^{(l)}(z)$ for $\forall \gamma \in [0, 1]$, is a Schur polynomial. According to this condition, a stability domain with an interior point $\boldsymbol{q}^{(l-1)}$ can be defined as $D_s = \{\boldsymbol{q}^{(l)} \mid R^{(l)}(z) \text{ is SPR}\}$. Note that the condition that $R^{(l)}(z)$ is SPR is equivalent to requiring that

$$\begin{aligned} & R^{(l)}(z) + R^{(l)}(z^{-1}) \\ &= \frac{Q^{(l)}(z)Q^{(l-1)}(z^{-1}) + Q^{(l-1)}(z)Q^{(l)}(z^{-1})}{Q^{(l-1)}(z)Q^{(l-1)}(z^{-1})} \end{aligned} \tag{33}$$

is real and positive on the unit circle. Since the denominator of (33) is always positive on the unit circle, it follows that the symmetric numerator polynomial of (33) must be positive on the unit circle for $\forall \omega \in [0, \pi]$, which can be cast as a linear matrix inequality (LMI) constraint independent of frequency ω (Dumitrescu & Niemistö, 2004). Here, the stability constraint $R^{(l)}(e^{j\omega})+R^{(l)}(e^{-j\omega}) > 0$ can be expressed in the form of linear inequality constraints as

$$\begin{aligned} & \mathrm{Re}\left\{Q^{(l-1)}(e^{-j\omega_i})\boldsymbol{\varphi}_2^T(e^{j\omega_i})\right\}\boldsymbol{q}^{(l)} \geq \nu - \mathrm{Re}\left\{Q^{(l-1)}(e^{j\omega_i})\right\} \\ & \omega_i \in [0, \pi], i = 1, \cdots, I \end{aligned} \tag{34}$$

where ν is a specified small positive number. If variable denominator is utilized in $H(z,t)$, the term $\boldsymbol{q}^{(l)T}\boldsymbol{\varphi}_2(e^{j\omega})$ in (34) should be replaced by $\boldsymbol{b}^{(l)T}\boldsymbol{u}_2(e^{j\omega},t)$. Thereby, (34) can be expressed as

$$\begin{aligned} &\mathrm{Re}\left\{Q^{(l-1)}(e^{-j\omega_i},t_j)\boldsymbol{u}_2^T(e^{j\omega_i},t_j)\right\}\boldsymbol{b}^{(l)} \geq \nu - \mathrm{Re}\left\{Q^{(l-1)}(e^{j\omega_i},t_j)\right\} \\ &\omega_i \in [0,\pi], i=1,\cdots,I; \quad t_j \in [-0.5,0.5],\ j=1,\cdots,J \end{aligned} \tag{35}$$

4. Gradient-based design of IIR VFD digital filters

In this section, a gradient-based design method for IIR VFD digital filters is presented. An initial design is first obtained by solving a SOCP problem, and a local search procedure is then applied to refine the design.

4.1 Initial design using SOCP

IIR VFD filter design using optimization is a non-convex problem and there could be many local minima on its error performance surface. Also, a large IIR VFD filter design problem involves many variables $(N+1)(K_1+1)+M(K_2+1)$. In order to obtain a good initial design that would lead to a satisfactory final design, consider the following initial design problem derived from (19) by applying the Levy's method (Levy, 1959) on $e(w,t)$ to obtain $e(w,t)Q(e^{jw},t)$ as

$$\begin{aligned} \min_{\boldsymbol{x}} \ J_1(\boldsymbol{x}) &= \int_0^{\alpha\pi}\int_{-0.5}^{0.5} W(\omega,t)\left|e(\omega,t)Q(e^{j\omega},t)\right|^2 dtd\omega \\ &= \boldsymbol{x}^T\boldsymbol{G}\boldsymbol{x} - 2\boldsymbol{x}^T\boldsymbol{g} + c \end{aligned} \tag{36}$$

where $\boldsymbol{G}$, $\boldsymbol{g}$, and c can be readily obtained by replacing the weighting function $W^{(l-1)}(\omega, t)$ of (22) in (26)-(28) by $W(\omega, t)$ of (19). Similar to (25)-(29), the design problem (36) can be transformed into the following SOCP problem as

$$\min \varepsilon \tag{37}$$

$$\text{s.t. } \left\|\bar{\boldsymbol{G}}\boldsymbol{x}\right\|^2 \leq 2\boldsymbol{x}^T\boldsymbol{g} + \varepsilon \tag{37a}$$

where the matrix $\bar{\boldsymbol{G}} = \boldsymbol{G}^{1/2}$.

4.2 Stability consideration

In order to guarantee the stability of a designed IIR VFD filter, stability constraints should be incorporated in (37). The linear stability constraints (34) or (35) can be directly incorporated into the design problem (37). Besides (34) or (35), the following strategy can also be employed to ensure the stability. It is known that by suppressing $\|q(t)\|^2$, the poles can be forced to move towards the origin in the z-plane (Zhao & Kwan, 2007). To do so, a regularization term defined in (38) below is introduced as

$$J_2(\boldsymbol{x}) = \int_{-0.5}^{0.5}\left\|\boldsymbol{q}(t)\right\|^2 dt = \sum_{m=1}^{M}\boldsymbol{b}_m^T\boldsymbol{V}_2\boldsymbol{b}_m = \boldsymbol{b}^T\boldsymbol{V}\boldsymbol{b} \tag{38}$$

where

$$\boldsymbol{V}_2 = \int_{-0.5}^{0.5} \boldsymbol{v}_2(t)\boldsymbol{v}_2^T(t)dt \tag{39}$$

$$\boldsymbol{V} = \begin{bmatrix} \boldsymbol{V}_2 & & & \\ & \boldsymbol{V}_2 & & \\ & & \ddots & \\ & & & \boldsymbol{V}_2 \end{bmatrix} \tag{40}$$

By combining $J_2(\boldsymbol{x})$ with the cost function $J_1(\mathrm{x})$ of (36) through a regularization coefficient β, the design problem (36) is then formulated as

$$\begin{aligned} \min_{\boldsymbol{x}} \quad & J_1(\boldsymbol{x}) + \beta J_2(\boldsymbol{x}) \\ & = \boldsymbol{x}^T \hat{\boldsymbol{G}}\, \boldsymbol{x} - 2\boldsymbol{x}^T \boldsymbol{g} + c \end{aligned} \tag{41}$$

where

$$\hat{\boldsymbol{G}} = \boldsymbol{G} + \begin{bmatrix} \boldsymbol{0}_{(N+1)(K_1+1)\times(N+1)(K_1+1)} & \boldsymbol{0}_{(N+1)(K_1+1)\times M(K_2+1)} \\ \boldsymbol{0}_{M(K_2+1)\times(N+1)(K_1+1)} & \beta \boldsymbol{V} \end{bmatrix} \tag{42}$$

In (42), $\boldsymbol{0}_{m\times n}$ represents a zero matrix of size m-by-n. The design problem (41) can then be formulated as a SOCP problem similar to (37) as

$$\min \ \hat{\varepsilon} \tag{43}$$

$$\text{s.t.} \ \left\| \tilde{\boldsymbol{G}}\boldsymbol{x} \right\|^2 \le 2\boldsymbol{x}^T \boldsymbol{g} + \hat{\varepsilon} \tag{43a}$$

where $\tilde{\boldsymbol{G}} = \hat{\boldsymbol{G}}^{1/2}$.

4.3 Local search

Although both the design problem (37) subject to stability constraints (34) or (35) and the design problem (43) are convex and can be efficiently solved, the obtained design in either case may not be a truly (locally) optimal design in the WLS sense, since the cost function $J_1(\boldsymbol{x})$ of (36) is not equivalent to the original one in (19). Therefore, a local search should be performed to locate the local optimum near the initial design (obtained by solving (37) with appropriate stability constraints (34) or (35) or by solving (43)). Here, a general-purpose gradient-based optimization algorithm (e.g., quasi-Newton) is employed to achieve a local optimal design. Normally, such an algorithm requires a designer to provide subroutines to calculate the function value and the gradient at a given point. Thus, the formulas to calculate the gradients of $J(\boldsymbol{x})$ defined in (19) can be derived as

$$\begin{aligned}\nabla_{\boldsymbol{a}} J(\boldsymbol{x}) &= \nabla_{\boldsymbol{a}} \left[\int_0^{\alpha\pi} \int_{-0.5}^{0.5} W(\omega,t) \left| e(\omega,t) \right|^2 dt d\omega \right] \\ &= 2 \int_0^{\alpha\pi} \int_{-0.5}^{0.5} W(\omega,t) \operatorname{Re} \left\{ \frac{e^*(\omega,t)}{Q(e^{j\omega},t)} \boldsymbol{u}_1(e^{j\omega},t) \right\} dt d\omega \end{aligned} \tag{44}$$

$$\begin{aligned}\nabla_{\boldsymbol{b}} J(\boldsymbol{x}) &= \nabla_{\boldsymbol{b}} \left[\int_0^{\alpha\pi} \int_{-0.5}^{0.5} W(\omega,t) \left| e(\omega,t) \right|^2 dt d\omega \right] \\ &= -2 \int_0^{\alpha\pi} \int_{-0.5}^{0.5} W(\omega,t) \operatorname{Re} \left\{ \frac{e^*(\omega,t) H(e^{j\omega},t)}{Q(e^{j\omega},t)} \boldsymbol{u}_2(e^{j\omega},t) \right\} dt d\omega \end{aligned} \tag{45}$$

In (44)-(45), the subscript * denotes complex conjugate operation. It is noted that if an initial design is stable, the IIR filter obtained by the local search is stable. It is because if any of the poles moves close to the unit circle, it will create a large approximation error; and in case the situation that a pole and a zero nearly cancel or cancel each other emerges, the error performance will degrade due to a reduced filter order. Since a gradient-based algorithm can only find local minima around an initial design, if pole-zero cancellation does not appear in an initial design, pole-zero cancellation is not likely to appear in the subsequent local search using a gradient-based algorithm. Furthermore, the step size of a gradient-based algorithm can be automatically adjusted to guarantee that the obtained filter in each iteration stays inside the stable domain. The above scheme works well in all our designs. In the designs, the optimization command 'fminunc' in MATLAB was adopted to perform the local search. The stability of a designed VdIIR VFD filter is ensured if its maximum pole radius is within the unity circle at each of the fractional delay values obtained from a dense grid of fractional delay $t \in [-0.5, 0.5]$. On the other hand, the stability of a designed FdIIR VFD filter can simply be checked by ensuring its maximum pole radius is within the unity circle.

5. Design specifications

In this section, four sets of filter examples are presented to demonstrate the effectiveness of the sequential and gradient-based design methods. For a fair comparison, at each of the four specified cutoff frequencies, all the three types (IIR, allpass, and FIR) of VFD filters are specified to have the same number of variable coefficients, i.e., $(N+1)(K_1+1)+M(K_2+1) = M_{AP}(K_1+1) = (L_{FIR}+1)(K_1+1)$, where M_{AP} and L_{FIR} denote, respectively, the filter order of an allpass VFD filter and the filter order of an FIR VFD filter. To achieve a good IIR VFD filter design based on a general IIR digital filter, the denominator order needs not be as high as the numerator order. Therefore, in each of the IIR VFD filter designs, the denominator order M is chosen to be 6 which is smaller than the corresponding numerator order N. The filter specifications of the IIR VFD filters with variable and fixed denominators are summarized in Table 1 whereas the design specifications of allpass and FIR VFD filters are summarized in Table 2.

α	(K_1, K_2)	(N, M, D)
0.9625	(5, 5)	(49, 6, 25), (49, 6, 28), (49, 6, 31)
	(5, 0)	(54, 6, 27), (54, 6, 30), (54, 6, 33)
0.9500	(5, 5)	(46, 6, 23), (46, 6, 26), (46, 6 29)
	(5, 0)	(51, 6, 26), (51, 6, 29), (51, 6 32)
0.9250	(5, 5)	(41, 6, 21), (41, 6, 24), (41, 6, 27)
	(5, 0)	(46, 6, 23), (46, 6, 26), (46, 6, 29)
0.9000	(5, 5)	(36, 6, 18), (36, 6, 21), (36, 6, 24)
	(5, 0)	(41, 6, 21), (41, 6, 24), (41, 6, 27)

Table 1. IIR VFD filter specifications (Keys: α: Normalized passband; K_1 (K_2): Numerator (Denominator) coefficient polynomial order; N (M): Numerator (Denominator) order; D: IIR mean group delay)

α	K_1	(M_{AP}, D_{AP})	(L_{FIR}, D_{FIR})
0.9625	5	(56, 56)	(55, 28)
0.9500	5	(53, 53)	(52, 26)
0.9250	5	(48, 48)	(47, 24)
0.9000	5	(43, 43)	(42, 21)

Table 2. Allpass and FIR VFD filter specifications (Keys: α: Normalized passband; K_1: Coefficient polynomial order; M_{AP}: Allpass order; D_{AP}: Allpass mean group delay; L_{FIR}: FIR order; D_{FIR}: FIR mean group delay)

The respective mean group delay is somehow related to (a) the numerator and denominator orders, N and M, for an IIR VFD filter; (b) the filter order M_{AP} of an allpass VFD filter; and (c) the filter order L_{FIR} of an FIR VFD filter. In Tables 1 and 2, the respective mean group delay is chosen as: (a) D = the round up value of $(N+M)/2$ for an IIR VFD filter; (b) D_{AP} = the filter order M_{AP} for an allpass VFD filter; and (c) D_{FIR} = the round up value of $L_{FIR}/2$ for an FIR VFD filter. The choice of mean group delay values $D = \lceil (N+M)/2 \rceil$ and $\lceil (N+M)/2 \rceil \pm 3$ shown in Table 1 for all the IIR VFD filter design methods allows a comparison of their relative performances in order to determine the best design method upon which its best mean group delay value that yields a minimum e_{rms} can be determined by simulations to be described in Section 6.2. The design results obtained by the proposed designs are compared with those of the IIR VFD filters with variable denominators designed by (ZK), the IIR VFD filters with fixed denominators designed by (KJ) and (TCK), the allpass VFD filters designed by (KJ) and (LCR), and the FIR VFD filters designed by (KJ) and (LD). For fair comparisons, the weighting function $W(\omega,t)$ in (19) and (36) is always set equal to 1 for $\forall \omega \in [0, \alpha\pi]$ and $\forall t \in [-0.5, 0.5]$. The relaxation constant λ used in (30) and the tolerance μ used in the stopping criterion (31) are chosen as 0.5 and 10^{-4}, respectively. The stability constraints (35) are imposed on 21×21 discrete points evenly distributed over the domain $[0, \pi] \times [-0.5, 0.5]$. For $K_2 = 0$, the stability constraints (34) are imposed on 21 frequency points, which are equally spaced over the range $[0, \pi]$. The parameter ν in (34) and (35) are chosen as 10^{-3}. The optimal value of β used in (46) is 10^{-10} (except for VdIIR VFD filters at $\alpha = 0.9625$, $\beta = 10^{-9}$; and for

FdIIR VFD filters at α = 0.9, β = 0). At each iteration, the SOCP problems in (29), (37) and (43) are solved using *SeDuMi* (Sturm, 1999) under MATLAB environment.

6. Performance analysis

6.1 Error measurements and stability check

To evaluate the performances of each designed VFD filter, the maximum absolute error e_{max}, and the normalized root-mean-squared (RMS) error e_{rms} of its (a) frequency responses, (b) magnitude responses, and (c) fractional group delay responses are adopted and they are defined, respectively, by

$$e_{max} = \max\left\{\left|e(\omega,t)\right|,\ \omega\in[0,\alpha\pi], t\in[-0.5,0.5]\right\} \tag{46}$$

$$e_{rms} = \left[\frac{\int_0^{\alpha\pi}\int_{-0.5}^{0.5}\left|e(\omega,t)\right|^2 dtd\omega}{\int_0^{\alpha\pi}\int_{-0.5}^{0.5}\left|H_d(\omega,t)\right|^2 dtd\omega}\right]^{1/2} \tag{47}$$

$$e_{max,1} = \max\left\{\left|e_{MAG}(\omega,t)\right|,\ \omega\in[0,\alpha\pi], t\in[-0.5,0.5]\right\} \tag{48}$$

$$e_{rms,1} = \left[\frac{\int_0^{\alpha\pi}\int_{-0.5}^{0.5}\left|e_{MAG}(\omega,t)\right|^2 dtd\omega}{\int_0^{\alpha\pi}\int_{-0.5}^{0.5}\left|H_d(\omega,t)\right|^2 dtd\omega}\right]^{1/2} \tag{49}$$

$$e_{max,2} = \max\left\{\left|e_{FGD}(\omega,t)\right|,\ \omega\in[0,\alpha\pi], t\in[-0.5,0.5]\right\} \tag{50}$$

$$e_{rms,2} = \left[\frac{\int_0^{\alpha\pi}\int_{-0.5}^{0.5}\left|e_{FGD}(\omega,t)\right|^2 dtd\omega}{\int_0^{\alpha\pi}\int_{-0.5}^{0.5} t^2 dtd\omega}\right]^{1/2} \tag{51}$$

where

$$e_{MAG}(\omega,t) = \left|H(e^{j\omega},t)\right| - \left|H_d(\omega,t)\right| \tag{52}$$

$$e_{FGD}(\omega,t) = \tau(\omega,t) - t \tag{53}$$

In (53), $\tau(\omega,t)$ denotes the actual fractional group delay of a designed VFD filter. Since the design problem is formulated in the WLS sense (see (19)), so the e_{rms} of the frequency responses is the most appropriate criterion for comparisons among different design methods. In case two designs have the same e_{rms}, other error measurements shall be compared. For each of the designed VdIIR VFD filters and AP VFD filters, a uniform grid consisting of 1001 discrete fractional delay values t were used to ensure all these 1001 VFD filters are stable. By checking individual maximum pole radius to be within the unity circle, each of the designed VFD filters has been verified to be stable.

6.2 IIR VFD filter performances

Based on the design specifications of Table 1, the error performances of the designed IIR VFD filters are summarized in Tables 3-4. The keywords adopted in Tables 3-4 are defined as follows: The "Sequential design" refers to the minimization problem defined by (29) subject to (a) stability inequality constraints (35) for VdIIR VFD filter design; and (b) stability inequality constraints (34) for FdIIR VFD filter design. The "Gradient-based design with (35)" refers to the minimization problem defined by (37) subject to stability inequality constraints (35) for an initial VdIIR VFD filter design, and followed by a local search. The "Gradient-based design with (34)" refers to the minimization problem defined by (37) subject to stability inequality constraints (34) for an initial FdIIR VFD filter design, and followed by a local search. The "Gradient-based design with (43)" refers to the minimization problem defined by (43) for an initial VdIIR or FdIIR VFD filter design, and followed by a local search. Within each of the four sets of designs, the relative e_{rms} (in frequency responses) performances are ranked from top to bottom as shown in Tables 3-4. The top performer of each IIR VFD design method in Tables 3-4 is listed in Table 5.

As shown in Table 5, the e_{rms} performances among the VdIIR VFD filters can be summarized as follows: The top performers for $0.95 \le \alpha \le 0.9625$ are the gradient-based designs with (35). The top performers for $0.9 \le \alpha \le 0.925$ are the gradient-based designs with (43). The bottom performer is the two-stage design of (ZK). The performance of the sequential designs (29) ranks at the middle between the designs of (ZK) and the gradient-based designs with (35) and with (43). As also shown in Table 5, the e_{rms} performances among the FdIIR VFD filters can be summarized as follows: The top performers for $0.925 \le \alpha \le 0.9625$ are the gradient-based designs with (43) but has an average performance for $\alpha = 0.9$. The top performer for $\alpha = 0.9$ is the gradient-based design with (34) which has close but lower performances than those of the gradient-based designs with (43) for $0.925 \le \alpha \le 0.95$. The bottom performer for $0.925 \le \alpha \le 0.9625$ is (TCK) but it ranks second among all the FdIIR VFD designs for $\alpha = 0.9$. Between (KJ) and the sequential design (29), the former ranks higher than those of the sequential designs (29) for $0.95 \le \alpha \le 0.9625$ but vice versa for $0.9 \le \alpha \le 0.925$. Comparing (KJ) and (TCK), the former yields better performances for $0.925 \le \alpha \le 0.9625$ but vice versa for $\alpha = 0.9$.

a	N	D	A	R	Freq. Responses		Mag. Responses		FGD Responses	
					e_{max} (dB)	e_{rms}	$e_{max,1}$(dB)	$e_{rms,1}$	$e_{max,2}$	$e_{rms,2}$
α_1	49	25	(29)	9	-35.490	1.892e-3	-37.360	1.289e-3	1.763	2.754e-1
			(35)	3	-50.347	3.683e-4	-50.402	2.923e-4	3.970e-1	6.042e-2
			(43)	4	-46.317	4.790e-4	-46.373	3.607e-4	5.621e-1	7.708e-2
			(ZK)	12	-11.622	2.766e-2	-12.295	2.402e-2	1.972	4.208e-1
		28	(29)	8	-40.026	1.403e-3	-40.664	1.036e-3	1.160	1.823e-1
			(35)	2	-50.808	3.444e-4	-51.710	2.318e-4	4.850e-1	7.108e-2
			(43)	5	-45.817	4.981e-4	-48.255	3.327e-4	6.545e-1	9.443e-2
			(ZK)	11	-12.042	2.623e-2	-13.067	2.268e-2	1.892	4.291e-1
		31	(29)	7	-42.041	8.851e-4	-42.698	6.840e-4	9.504e-1	1.431e-1
			(35)	1	-52.436	2.890e-4	-53.731	1.833e-4	4.442e-1	6.963e-2
			(43)	6	-45.492	5.203e-4	-46.819	3.439e-4	6.152e-1	1.034e-1
			(ZK)	10	-12.674	2.460e-2	-13.590	2.110e-2	1.797	4.203e-1
α_2	46	23	(29)	9	-43.309	8.175e-4	-46.118	5.256e-4	6.791e-1	1.095e-1
			(35)	5	-57.964	1.563e-4	-57.970	1.230e-4	1.561e-1	2.346e-2
			(43)	6	-55.398	2.194e-4	-56.439	1.629e-4	2.370e-1	3.347e-2
			(ZK)	10	-17.857	1.511e-2	-18.471	1.328e-2	1.097	2.441e-1
		26	(29)	8	-48.237	4.151e-4	-50.465	2.946e-4	3.830e-1	6.093e-2
			(35)	3	-59.298	1.354e-4	-60.759	9.100e-5	1.680e-1	2.487e-2
			(43)	4	-59.500	1.442e-4	-59.567	1.025e-4	1.855e-1	2.446e-2
			(ZK)	11	-17.735	1.531e-2	-18.573	1.340e-2	1.021	2.346e-1
		29	(29)	7	-48.984	3.667e-4	-49.148	2.845e-4	3.047e-1	4.843e-2
			(35)	1	-60.500	1.171e-4	-63.434	7.782e-5	1.400e-1	2.453e-2
			(43)	2	-59.982	1.310e-4	-60.924	9.276e-5	1.434e-1	2.400e-2
			(ZK)	12	-11.036	2.871e-2	-12.351	2.526e-2	1.702	3.513e-1
α_3	41	21	(29)	9	-57.865	1.108e-4	-61.693	6.780e-5	1.306e-1	1.993e-2
			(35)	5	-62.965	5.007e-5	-63.189	3.882e-5	5.270e-2	7.486e-3
			(43)	6	-64.763	6.303e-5	-67.058	4.233e-5	7.008e-2	1.016e-2
			(ZK)	10	-18.100	1.752e-2	-18.330	1.493e-2	4.667e-1	1.575e-1
		24	(29)	7	-60.523	8.940e-5	-60.973	6.550e-5	9.716e-2	1.449e-2
			(35)	4	-66.111	4.390e-5	-67.968	3.004e-5	5.477e-2	8.191e-3
			(43)	3	-69.381	3.348e-5	-70.084	2.327e-5	4.344e-2	6.336e-3
			(ZK)	11	-15.405	1.998e-2	-15.883	1.767e-2	6.691e-1	1.745e-1
		27	(29)	8	-59.811	9.295e-5	-59.859	7.225e-5	7.450e-2	1.322e-2
			(35)	2	-67.930	3.255e-5	-72.267	2.048e-5	4.415e-2	7.135e-3
			(43)	1	-75.807	1.269e-5	-78.312	8.311e-6	2.229e-2	2.984e-3
			(ZK)	12	-13.440	2.520e-2	-14.190	2.242e-2	1.020	2.197e-1

α_4	36	18	(29)	7	-70.872	3.336e-5	-74.955	2.250e-5	2.631e-2	4.264e-3
			(35)	9	-71.177	3.592e-5	-71.466	2.760e-5	2.270e-2	3.510e-3
			(43)	4	-71.255	2.661e-5	-73.122	1.942e-5	2.182e-2	3.217e-3
			(ZK)	11	-20.667	1.381e-2	-20.070	1.113e-2	2.332e-1	1.109e-1
		21	(29)	6	-71.817	3.311e-5	-73.389	2.411e-5	2.564e-2	3.895e-3
			(35)	5	-72.620	2.730e-5	-73.472	1.881e-5	2.110e-2	3.541e-3
			(43)	2	-79.979	7.880e-6	-83.184	5.360e-6	8.086e-3	1.170e-3
			(ZK)	10	-21.880	1.139e-2	-22.079	9.317e-3	2.680e-1	1.033e-1
		24	(29)	8	-71.882	3.488e-5	-72.448	2.545e-5	1.982e-2	3.541e-3
			(35)	3	-75.763	2.294e-5	-77.805	1.494e-5	2.183e-2	3.434e-3
			(43)	1	-83.278	6.257e-6	-85.250	4.068e-6	8.721e-3	1.314e-3
			(ZK)	12	-14.311	2.847e-2	-14.477	2.483e-2	5.477e-1	1.958e-1

Table 3. Performances of VdIIR VFD filters (Keys: α_1= 0.9625, α_2= 0.95, α_3= 0.925, α_4= 0.9; A: Design method; (29): Sequential design; (35): Gradient-based design with (35); (43): Gradient-based design with (43); (ZK): (Zhao & Kwan, 2007); R: Rank; FGD: Fractional group delay)

a	N	D	A	R	Freq. Responses		Mag. Responses		FGD Responses	
					e_{max}	e_{rms}	$e_{max,1}$(dB)	$e_{rms,1}$	$e_{max,2}$	$e_{rms,2}$
α_1	54	27	(29)	12	-38.000	1.426e-3	-40.368	9.325e-4	1.556	2.398e-1
			(34)	6	-51.464	2.796e-4	-52.628	2.229e-4	3.141e-1	4.812e-2
			(43)	5	-49.821	2.791e-4	-49.826	2.345e-4	2.523e-1	4.390e-2
			(KJ)	9	-39.632	5.615e-4	-39.696	4.623e-4	8.980e-1	1.365e-1
			(TCK)	15	-30.303	2.429e-3	-31.218	1.974e-3	3.359	5.846e-1
		30	(29)	11	-42.034	9.887e-4	-43.963	7.094e-4	1.014	1.559e-1
			(34)	4	-50.852	2.683e-4	-53.605	1.810e-4	3.932e-1	6.088e-2
			(43)	3	-49.940	2.663e-4	-51.336	1.906e-4	3.675e-1	5.526e-2
			(KJ)	7	-40.645	5.044e-4	-41.407	3.952e-4	1.010	1.446e-1
			(TCK)	14	-31.333	2.206e-3	-34.075	1.415e-3	3.364	6.026e-1
		33	(29)	10	-43.634	6.475e-4	-45.398	4.989e-4	8.047e-1	1.196e-1
			(34)	2	-50.271	2.647e-4	-54.681	1.649e-4	4.254e-1	6.933e-2
			(43)	1	-58.117	1.360e-4	-59.459	1.055e-4	1.553e-1	2.391e-2
			(KJ)	8	-40.973	5.101e-4	-42.615	3.681e-4	1.143	1.668e-1
			(TCK)	13	-33.233	1.793e-3	-38.764	8.176e-4	2.853	5.160e-1
α_2	51	26	(29)	12	-46.106	4.757e-4	-49.348	3.021e-4	4.745e-1	7.514e-2
			(34)	9	-56.847	1.423e-4	-59.984	1.015e-4	1.334e-1	2.122e-2
			(43)	3	-60.282	1.172e-4	-62.605	9.084e-5	8.234e-2	1.344e-2
			(KJ)	5	-55.680	1.241e-4	-58.979	8.890e-5	2.465e-1	3.491e-2
			(TCK)	15	-38.816	8.603e-4	-38.917	7.661e-4	1.178	1.856e-1

		29	(29)	11	-49.943	2.895e-4	-52.464	2.166e-4	2.821e-1	4.396e-2
			(34)	8	-55.870	1.386e-4	-63.233	8.848e-5	1.524e-1	2.632e-2
			(43)	2	-60.166	1.051e-4	-64.946	7.397e-5	8.715e-2	1.359e-2
			(KJ)	4	-56.758	1.193e-4	-59.001	8.726e-5	1.691e-1	2.528e-2
			(TCK)	14	-40.109	8.059e-4	-42.311	5.295e-4	1.314	2.294e-1
		32	(29)	10	-51.166	2.425e-4	-52.046	1.934e-4	2.142e-1	3.369e-2
			(34)	7	-55.703	1.382e-4	-61.363	9.540e-5	1.556e-1	2.623e-2
			(43)	1	-58.723	1.018e-4	-65.813	7.060e-5	1.013e-1	1.683e-2
			(KJ)	6	-55.965	1.287e-4	-55.998	9.835e-5	1.528e-1	2.498e-2
			(TCK)	13	-41.867	6.935e-4	-48.144	3.326e-4	1.023	1.822e-1
α_3	46	23	(29)	12	-56.063	1.152e-4	-60.966	7.670e-5	1.237e-1	1.812e-2
			(34)	3	-59.700	7.518e-5	-67.140	5.471e-5	4.434e-2	6.868e-3
			(43)	4	-61.491	7.567e-5	-66.350	5.607e-5	3.709e-2	5.591e-3
			(KJ)	10	-58.608	9.039e-5	-62.759	6.328e-5	8.504e-2	1.145e-2
			(TCK)	13	-55.650	1.372e-4	-56.367	1.175e-4	1.242e-1	1.750e-2
		26	(29)	7	-60.462	8.640e-5	-64.213	6.376e-5	6.447e-2	9.586e-3
			(34)	6	-59.137	8.352e-5	-66.130	5.871e-5	6.708e-2	9.784e-3
			(43)	2	-61.693	7.237e-5	-68.770	5.183e-5	3.782e-2	5.498e-3
			(KJ)	9	-61.008	8.814e-5	-63.846	6.359e-5	5.162e-2	7.425e-3
			(TCK)	14	-54.098	1.536e-4	-55.608	1.325e-4	2.001e-1	2.945e-2
		29	(29)	5	-61.122	8.273e-5	-64.300	6.255e-5	5.129e-2	7.660e-3
			(34)	11	-58.753	9.176e-5	-65.279	6.558e-5	7.955e-2	1.131e-2
			(43)	1	-60.702	7.065e-5	-69.047	5.209e-5	3.796e-2	5.501e-3
			(KJ)	8	-62.337	8.694e-5	-64.720	6.295e-5	4.210e-2	6.087e-3
			(TCK)	15	-54.170	1.639e-4	-57.739	8.782e-5	2.696e-1	4.845e-2
α_4	41	21	(29)	8	-63.290	6.478e-5	-68.632	4.749e-5	2.587e-2	3.957e-3
			(34)	1	-62.541	5.875e-5	-71.768	4.111e-5	2.003e-2	3.037e-3
			(43)	5	-64.151	6.078e-5	-71.767	4.448e-5	1.876e-2	2.673e-3
			(KJ)	11	-66.316	7.136e-5	-70.722	5.197e-5	7.839e-3	1.202e-3
			(TCK)	2	-64.839	5.948e-5	-71.691	4.386e-5	2.400e-2	3.768e-3
		24	(29)	6	-63.812	6.103e-5	-69.829	4.557e-5	1.439e-2	2.480e-3
			(34)	3	-61.956	5.978e-5	-70.458	4.250e-5	2.073e-2	3.177e-3
			(43)	4	-63.959	6.049e-5	-69.984	4.491e-5	1.615e-2	2.565e-3
			(KJ)	12	-65.803	7.137e-5	-70.716	5.194e-5	1.140e-2	1.686e-3
			(TCK)	14	-63.694	8.469e-5	-64.780	5.867e-5	6.538e-2	1.150e-2
		27	(29)	7	-64.154	6.237e-5	-69.549	4.676e-5	1.283e-2	2.222e-3
			(34)	9	-62.223	6.748e-5	-66.374	4.933e-5	1.815e-2	3.434e-3

			(43)	10	-62.973	7.050e-5	-65.414	5.395e-5	1.670e-2	3.412e-3
			(KJ)	13	-66.208	7.147e-5	-70.498	5.203e-5	1.101e-2	1.632e-3
			(TCK)	15	-58.427	1.680e-4	-58.631	1.203e-4	7.196e-2	1.499e-2

Table 4. Performances of FdIIR VFD filters (Keys: α_1= 0.9625, α_2= 0.95, α_3= 0.925, α_4= 0.9; A: Design method; (29): Sequential design; (34): Gradient-based design with (34); (43): Gradient-based design with (43); (KJ): (Kwan & Jiang, 2009a); (TCK): (Tsui et al., 2007); R: Rank; FGD: Fractional group delay)

α		VdIIR				FdIIR				
		(29)	(35)	(43)	(ZK)	(29)	(34)	(43)	(KJ)	(TCK)
α_1	e_{rms}	8.851e-4	2.890e-4	4.790e-4	2.460e-2	6.475e-4	2.647e-4	1.360e-4	5.044e-4	1.793e-3
	R	3	1	2	4	4	2	1	3	5
α_2	e_{rms}	3.667e-4	1.171e-4	1.310e-4	1.511e-2	2.425e-4	1.382e-4	1.018e-4	1.193e-4	6.935e-4
	R	3	1	2	4	4	3	1	2	5
α_3	e_{rms}	8.940e-5	3.255e-5	1.269e-5	1.752e-2	8.273e-5	7.518e-5	7.065e-5	8.694e-5	1.372e-4
	R	3	2	1	4	3	2	1	4	5
α_4	e_{rms}	3.311e-5	2.294e-5	6.257e-6	1.139e-2	6.103e-5	5.875e-5	6.049e-5	7.136e-5	5.948e-5
	R	3	2	1	4	4	1	3	5	2

Table 5. Top-performed (e_{rms}) VFD filters from Tables 3-4 (Keys: α_1= 0.9625, α_2= 0.95, α_3= 0.925, α_4= 0.9; (ZK): (Zhao & Kwan, 2007); (KJ): (Kwan & Jiang, 2009a); (TCK): (Tsui et al., 2007); R: Rank)

6.3 Allpass and FIR VFD filter performances

The error performances of the AP VFD filters designed by (KJ) and (LCR) and the FIR VFD filters designed by (KJ) and (LD) are summarized in Table 6. In general, the two AP VFD filters achieve e_{rms} improvements over the two FIR VFD filters (except for (LD) at α = 0.9625). The top e_{rms} performances of the AP VFD filters are (KJ) for $0.925 \le \alpha \le 0.9625$ and (LCR) for α = 0.9.

6.4 Optimal gradient-based designs with (43)

It can be observed in Tables 3-4 that the error performances of VdIIR and FdIIR VFD filters at any specified cutoff frequency is a function of the mean group delay value D. To investigate this property further, consider the case of the gradient-based design with (43) in Table 5 in which it ranks top among VdIIR VFD filters for $0.9 \le \alpha \le 0.925$ and ranks top among FdIIR VFD filters for $0.925 \le \alpha \le 0.9625$. For each of the four cutoff frequencies, the error performances of the gradient-based designs with (43) for VdIIR and FdIIR VFD filters versus mean group delay D (at a step size of 3) are, respectively, summarized in Tables 7-8 and their corresponding e_{rms} values versus D are plotted in Figs. 1-8. From Tables 7-8, their mean group delay values D that yield minimum e_{rms} values are summarized in Table 9. For comparisons, the e_{rms} performances of the AP and FIR VFD filters from Table 6 are also listed under Table 9. The magnitude responses and group delay responses of the widest

band designs at α = 0.9625 obtained by the VdIIR and FdIIR VFD filters shown in Table 9 are plotted in Figs. 9-12.

a	OD	A/F	Freq. Responses		Mag. Responses		FGD Responses	
			e_{max} (dB)	e_{rms}	$e_{max,1}$(dB)	$e_{rms,1}$	$e_{max,2}$	$e_{rms,2}$
a_1	56, 56	A(KJ)	-40.677	3.246e-4	N.A.	N.A.	1.980	1.717e-1
		A(LCR)	-24.604	9.309e-3	N.A.	N.A.	5.920e-1	1.374e-1
	55, 28	F(KJ)	2.798	8.242e-1	-24.807	3.048e-3	2.117	1.761
		F(LD)	-31.994	3.573e-3	-31.997	2.933e-3	1.548	3.248e-1
a_2	53, 53	A(KJ)	-61.643	5.626e-5	N.A.	N.A.	4.437e-1	3.779e-2
		A(LCR)	-55.710	2.258e-4	N.A.	N.A.	8.224e-2	2.181e-2
	52, 26	F(KJ)	-32.726	1.493e-3	-32.770	1.216e-3	8.027e-1	1.633e-1
		F(LD)	-38.421	1.552e-3	-38.432	1.229e-3	6.470e-1	1.459e-1
a_3	48, 48	A(KJ)	-70.691	1.264e-5	N.A.	N.A.	2.011e-2	1.745e-3
		A(LCR)	-73.920	1.265e-5	N.A.	N.A.	2.991e-3	9.069e-4
	47, 24	F(KJ)	2.474	7.957e-1	-42.609	3.731e-4	7.122e-1	1.732
		F(LD)	-50.268	3.654e-4	-50.411	2.917e-4	1.802e-1	3.536e-2
a_4	43, 43	A(KJ)	-80.513	4.987e-6	N.A.	N.A.	5.892e-3	5.193e-4
		A(LCR)	-84.237	4.119e-6	N.A.	N.A.	3.870e-4	1.044e-4
	42, 21	F(KJ)	-53.561	1.310e-4	-53.810	1.027e-4	7.986e-2	1.609e-2
		F(LD)	-59.247	1.354e-4	-59.572	1.015e-4	5.479e-2	1.223e-2

Table 6. Performances of allpass and FIR VFD filters (Keys: α_1= 0.9625, α_2= 0.95, α_3= 0.925, α_4= 0.9; OD: Filter order and mean group delay (M_{AP}, D_{AP}) or (L_{FIR}, D_{FIR}); A: Allpass design, F: FIR design; (KJ): (Kwan & Jiang, 2009a); (LCR): (Lee et al., 2008); (LD): (Lu & Deng, 1999); FGD: Fractional group delay)

The relationship between numerator and denominator orders, and optimal mean group delay of a VdIIR or FdIIR VFD filter is a subject of interest. Table 10 summarizes such relationships among those VdIIR and FdIIR VDF filters listed in Table 9. It can be observed from Table 10 that as α changes from $0.9 \le \alpha \le 0.9625$, the ratio $D/(N+M)$ changes from 0.64 to 0.67 for VdIIR VFD filters, and changes from 0.57 to 0.55 for FdIIR VFD filters. Also, as seen from Figs. 1-8, for the higher wideband side with α = 0.9625 and 0.95, there is a mean group delay value that yields a minimum e_{rms} value; but for the lower wideband side with α = 0.925 and 0.9, each of the mean group delay curves shows that e_{rms} becomes lower much earlier at smaller D before reaching its minimum e_{rms} value. In other words, the mean group delay requirement is lower for lower wideband cutoff frequencies. From Table 10, in general, the VdIIR VFD filters require slightly higher optimal mean group delay values D than those of the corresponding FdIIR VFD filters.

a	N	D	R	Freq. Responses		Mag. Responses		*FGD* Responses	
				e_{max} (dB)	e_{rms}	$e_{max,1}$(dB)	$e_{rms,1}$	$e_{max,2}$	$e_{rms,2}$
a_1	49	25	6	-46.317	4.790e-4	-46.373	3.607e-4	5.621e-1	7.708e-2
		28	7	-45.817	4.981e-4	-48.255	3.327e-4	6.545e-1	9.443e-2
		31	8	-45.492	5.203e-4	-46.819	3.439e-4	6.152e-1	1.034e-1
		34	3	-55.689	1.709e-4	-56.650	1.203e-4	3.135e-1	4.301e-2
		37	1	-56.746	1.157e-4	-56.792	8.227e-5	2.371e-1	3.090e-2
		40	2	-54.753	1.333e-4	-55.272	8.621e-5	2.725e-1	3.913e-2
		43	4	-52.061	1.811e-4	-54.511	1.181e-4	3.634e-1	5.468e-2
		46	5	-48.664	2.877e-4	-48.979	2.016e-4	3.676e-1	6.420e-2
a_2	46	23	7	-55.398	2.194e-4	-56.439	1.629e-4	2.370e-1	3.347e-2
		26	6	-59.500	1.442e-4	-59.567	1.025e-4	1.855e-1	2.446e-2
		29	5	-59.982	1.310e-4	-60.924	9.276e-5	1.434e-1	2.400e-2
		32	2	-63.424	6.157e-5	-66.513	4.168e-5	1.025e-1	1.451e-2
		35	1	-64.515	5.514e-5	-67.411	3.558e-5	1.019e-1	1.364e-2
		38	3	-62.722	6.798e-5	-63.918	4.290e-5	1.184e-1	1.767e-2
		41	4	-57.588	9.448e-5	-57.757	7.247e-5	1.200e-1	1.731e-2
		44	8	-48.195	2.999e-4	-52.186	2.194e-4	5.620e-1	5.862e-2
a_3	41	18	8	-49.959	3.716e-4	-50.563	2.537e-4	2.966e-1	4.916e-2
		21	6	-64.763	6.303e-5	-67.058	4.233e-5	7.008e-2	1.016e-2
		24	5	-69.381	3.348e-5	-70.084	2.327e-5	4.344e-2	6.336e-3
		27	2	-75.807	1.269e-5	-78.312	8.311e-6	2.229e-2	2.984e-3
		30	1	-75.789	1.082e-5	-80.087	6.474e-6	2.048e-2	3.090e-3
		33	3	-71.425	1.823e-5	-71.675	1.433e-5	2.420e-2	3.420e-3
		36	4	-67.853	2.618e-5	-69.170	1.809e-5	3.759e-2	5.315e-3
		39	7	-59.463	7.159e-5	-61.018	5.770e-5	1.011e-1	1.101e-2
a_4	36	12	8	-54.423	3.608e-4	-54.631	2.655e-4	2.113e-1	3.317e-2
		15	7	-62.453	1.158e-4	-64.365	8.504e-5	7.312e-2	1.147e-2
		18	6	-71.255	2.661e-5	-73.122	1.942e-5	2.182e-2	3.217e-3
		21	3	-79.979	7.880e-6	-83.184	5.360e-6	8.086e-3	1.170e-3
		24	2	-83.278	6.257e-6	-85.250	4.068e-6	8.721e-3	1.314e-3
		27	1	-81.501	5.606e-6	-82.356	4.315e-6	6.449e-3	9.108e-4
		30	4	-76.734	8.225e-6	-82.492	5.195e-6	1.332e-2	1.626e-3
		33	5	-68.507	2.048e-5	-73.101	1.519e-5	2.204e-2	3.328e-3

Table 7. Performances of gradient-based design (43) of VdIIR VFD filters versus mean group delay (Keys: α_1= 0.9625, α_2= 0.95, α_3= 0.925, α_4= 0.9; R: Rank; FGD: Fractional group delay)

a	N	D	R	Freq. Responses		Mag. Responses		FGD Responses	
				e_{max} (dB)	e_{rms}	$e_{max,1}$(dB)	$e_{rms,1}$	$e_{max,2}$	$e_{rms,2}$
a_1	54	24	9	-47.551	4.030e-4	-48.815	3.254e-4	3.946e-1	6.066e-2
		27	8	-49.821	2.791e-4	-49.826	2.345e-4	2.523e-1	4.390e-2
		30	7	-49.940	2.663e-4	-51.336	1.906e-4	3.675e-1	5.526e-2
		33	1	-58.117	1.360e-4	-59.459	1.055e-4	1.553e-1	2.391e-2
		36	2	-54.776	1.581e-4	-56.752	1.100e-4	2.200e-1	3.225e-2
		39	3	-53.351	1.695e-4	-58.289	1.097e-4	3.108e-1	4.832e-2
		42	4	-52.767	1.852e-4	-57.168	1.246e-4	3.521e-1	5.312e-2
		45	5	-51.723	2.027e-4	-54.003	1.500e-4	3.394e-1	4.971e-2
		48	6	-50.532	2.165e-4	-53.051	1.745e-4	3.007e-1	4.414e-2
a_2	51	23	7	-57.352	1.585e-4	-57.948	1.258e-4	1.085e-1	1.823e-2
		26	4	-60.282	1.172e-4	-62.605	9.084e-5	8.234e-2	1.344e-2
		29	2	-60.166	1.051e-4	-64.946	7.397e-5	8.715e-2	1.359e-2
		32	1	-58.723	1.018e-4	-65.813	7.060e-5	1.013e-1	1.683e-2
		35	3	-56.737	1.073e-4	-63.980	7.180e-5	1.307e-1	1.956e-2
		38	5	-56.078	1.210e-4	-60.347	8.811e-5	1.470e-1	2.142e-2
		41	6	-57.176	1.354e-4	-58.376	1.015e-4	1.199e-1	1.825e-2
		44	8	-54.520	1.590e-4	-57.346	1.155e-4	1.488e-1	2.299e-2
		47	9	-51.036	2.173e-4	-58.471	1.441e-4	3.066e-1	5.044e-2
a_3	46	17	9	-54.883	1.565e-4	-56.964	1.190e-4	1.131e-1	1.781e-2
		20	8	-60.232	7.723e-5	-65.677	5.865e-5	3.142e-2	5.028e-3
		23	5	-61.491	7.567e-5	-66.350	5.607e-5	3.709e-2	5.591e-3
		26	2	-61.693	7.237e-5	-68.770	5.183e-5	3.782e-2	5.498e-3
		29	1	-60.702	7.065e-5	-69.047	5.209e-5	3.796e-2	5.501e-3
		32	3	-62.120	7.440e-5	-66.268	5.689e-5	2.962e-2	4.939e-3
		35	4	-60.883	7.454e-5	-66.131	5.552e-5	4.267e-2	6.465e-3
		38	7	-59.235	7.703e-5	-67.887	5.477e-5	6.825e-2	1.023e-2
		41	6	-58.976	7.603e-5	-66.870	5.497e-5	6.936e-2	1.007e-2
a_4	41	12	9	-55.792	1.883e-4	-58.359	1.342e-4	1.093e-1	1.991e-2
		15	8	-62.408	7.731e-5	-65.923	5.838e-5	3.030e-2	5.618e-3
		18	2	-63.307	5.875e-5	-71.407	4.177e-5	1.061e-2	1.921e-3
		21	5	-64.151	6.078e-5	-71.767	4.448e-5	1.876e-2	2.673e-3
		24	4	-63.959	6.049e-5	-69.984	4.491e-5	1.615e-2	2.565e-3
		27	1	-63.586	5.820e-5	-70.713	4.244e-5	9.738e-3	1.712e-3
		30	3	-61.756	5.975e-5	-70.908	4.170e-5	2.336e-2	3.916e-3
		33	6	-62.236	6.151e-5	-70.075	4.376e-5	3.241e-2	4.699e-3
		36	7	-61.444	6.189e-5	-68.939	4.454e-5	2.113e-2	3.729e-3

Table 8. Performances of gradient-based design (43) of FdIIR VFD filters versus mean group delay (Keys: α_1= 0.9625, α_2= 0.95, α_3= 0.925, α_4= 0.9; R: Rank; FGD: Fractional group delay)

α		VdIIR	FdIIR	AP		FIR	
		(43)	(43)	(KJ)	(LCR)	(KJ)	(LD)
α_1	D	37	33	56	56	28	28
	e_{rms}	1.157e-4	1.360e-4	3.246e-4	9.309e-3	8.242e-1	3.573e-3
α_2	D	35	32	53	53	26	26
	e_{rms}	5.514e-5	1.018e-4	5.626e-5	2.258e-4	1.493e-3	1.552e-3
α_3	D	30	29	48	48	24	24
	e_{rms}	1.082e-5	7.065e-5	1.264e-5	1.265e-5	7.957e-1	3.654e-4
α_4	D	27	27	43	43	21	21
	e_{rms}	5.606e-6	5.820e-5	4.987e-6	4.119e-6	1.310e-4	1.354e-4

Table 9. Performances (e_{rms}) of VFD filters selected from Tables 6-8 (Keys: α_1= 0.9625, α_2= 0.95, α_3= 0.925, α_4= 0.9; (KJ): (Kwan & Jiang, 2009a); (LCR): (Lee et al., 2008); (LD): (Lu & Deng, 1999))

	α	D	N	M	$N+M$	$D/(N+M)$
VdIIR	α_1	37	49	6	55	0.6727
	α_2	35	46	6	52	0.6731
	α_3	30	41	6	47	0.6383
	α_4	27	36	6	42	0.6429
FdIIR	α_1	33	54	6	60	0.5500
	α_2	32	51	6	57	0.5614
	α_3	29	46	6	52	0.5577
	α_4	27	41	6	47	0.5745

Table 10. D/(N+M) for IIR VFD filters (Keys: α_1= 0.9625, α_2= 0.95, α_3= 0.925, α_4= 0.9)

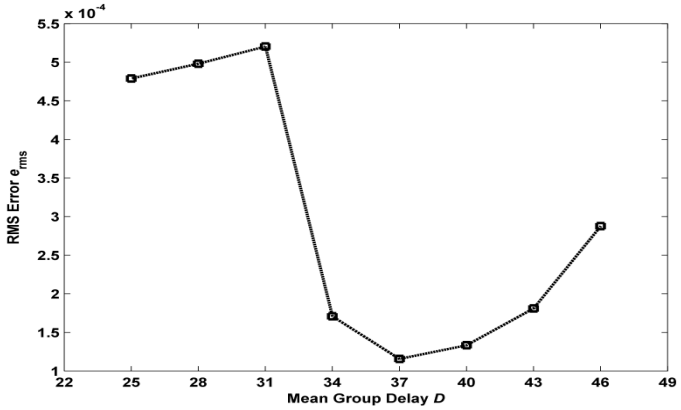

Fig. 1. e_{rms} versus mean group delay D (VdIIR VFD filter, a = 0.9625, N = 49, M = 6)

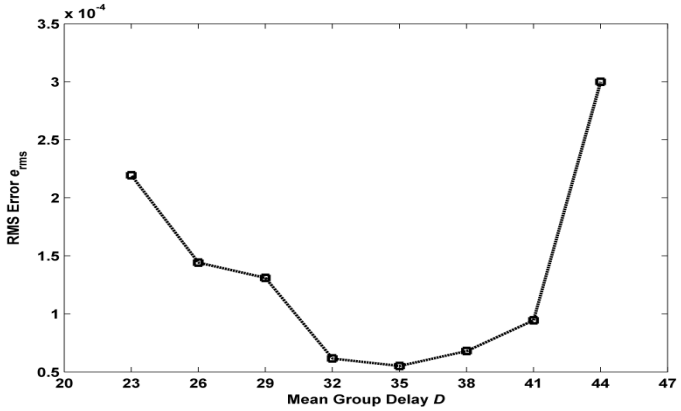

Fig. 2. e_{rms} versus mean group delay D (VdIIR VFD filter, a = 0.95, N = 46, M = 6)

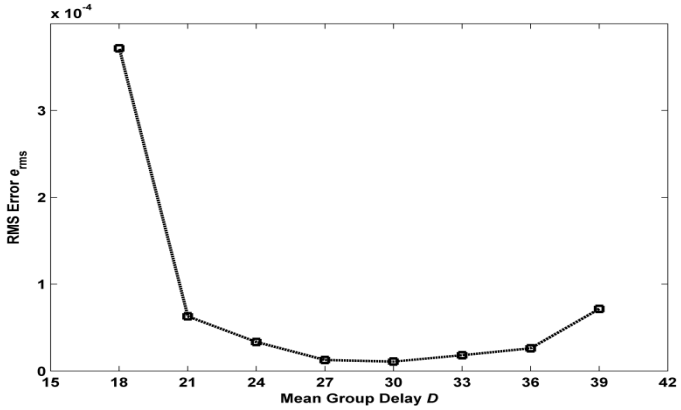

Fig. 3. e_{rms} versus mean group delay D (VdIIR VFD filter, a = 0.925, N = 41, M = 6)

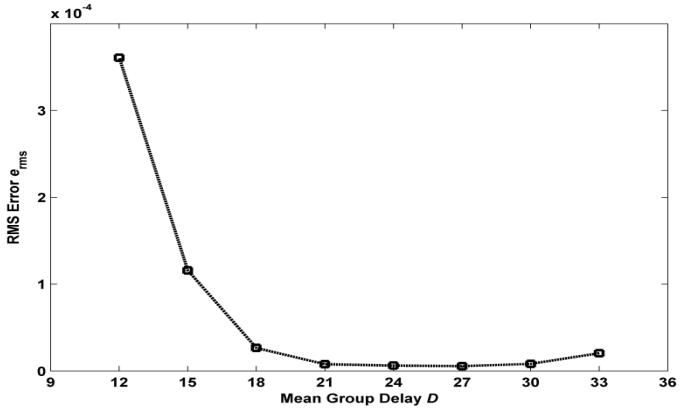

Fig. 4. e_{rms} versus mean group delay D (VdIIR VFD filter, a = 0.90, N = 36, M = 6)

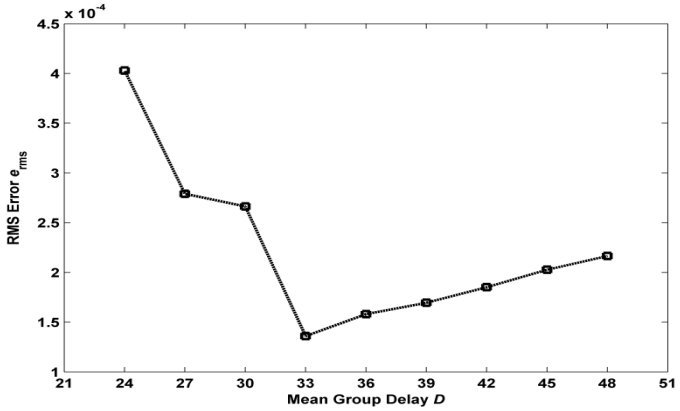

Fig. 5. e_{rms} versus mean group delay D (FdIIR VFD filter, a = 0.9625, N = 54, M = 6)

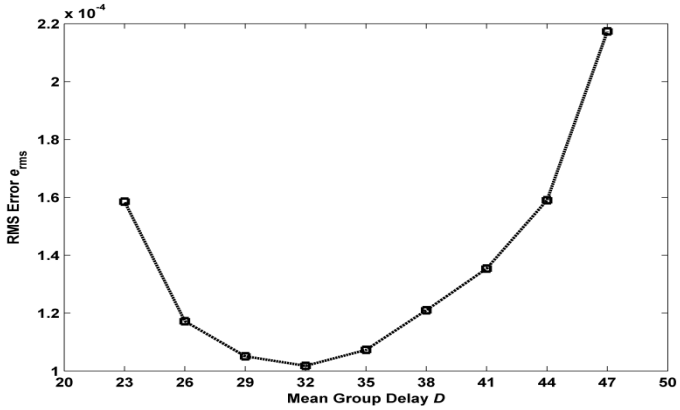

Fig. 6. e_{rms} versus mean group delay D (FdIIR VFD filter, a = 0.95, N = 51, M = 6)

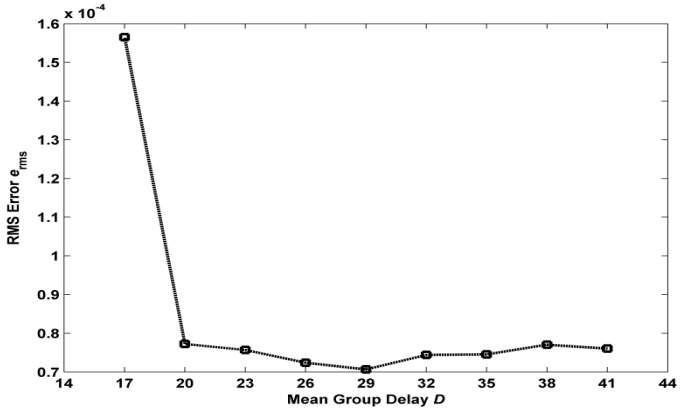

Fig. 7. e_{rms} versus mean group delay D (FdIIR VFD filter, a = 0.925, N = 46, M = 6)

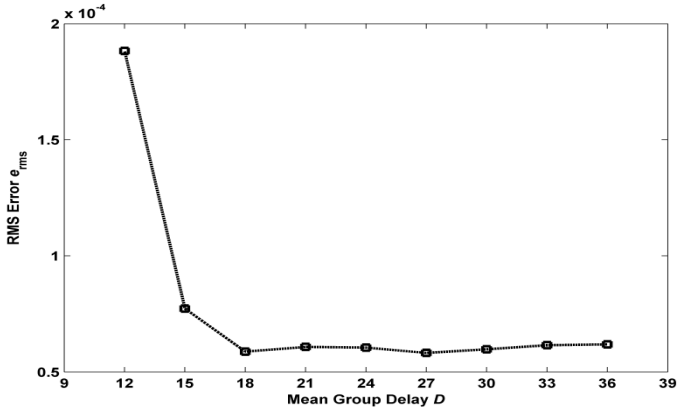

Fig. 8. e_{rms} versus mean group delay D (FdIIR VFD filter, a = 0.90, N = 41, M = 6)

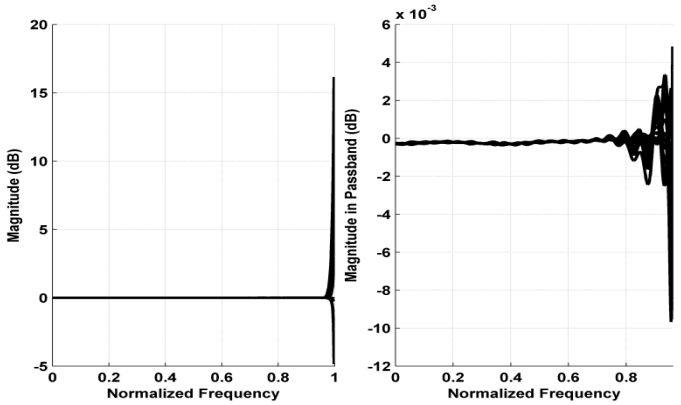

Fig. 9. Magnitude responses of VdIIR VFD filter obtained by gradient-based design method with (43) (a = 0.9625, N = 49, M = 6, D = 37)

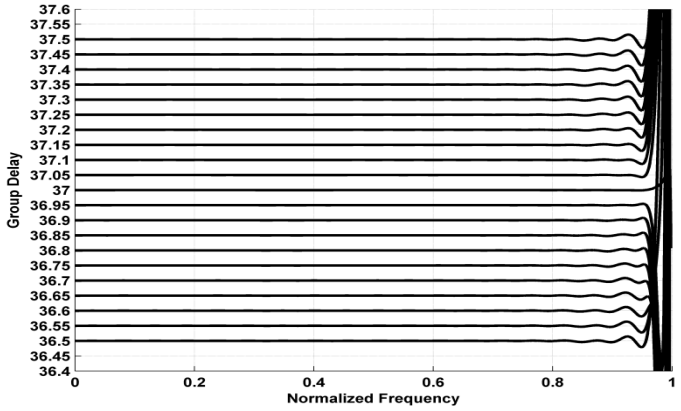

Fig. 10. Group delay responses of VdIIR VFD filter obtained by gradient-based design method with (43) (a = 0.9625, N = 49, M = 6, D = 37)

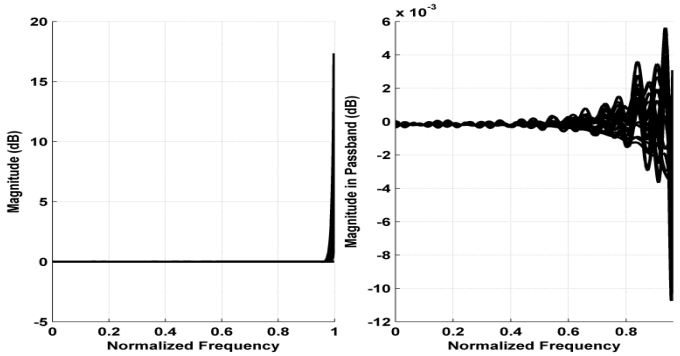

Fig. 11. Magnitude responses of FdIIR VFD filter obtained by gradient-based design method with (43) (a = 0.9625, N = 54, M = 6, D = 33)

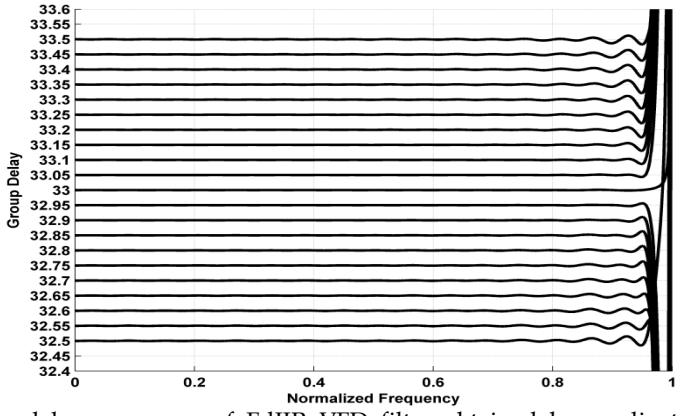

Fig. 12. Group delay responses of FdIIR VFD filter obtained by gradient-based design method with (43) (a = 0.9625, N = 54, M = 6, D = 33)

6.5 Overall IIR, allpass, and FIR VFD filter performances

To facilitate explanation in this sub-section, (29), (34), (35), (43) denote different proposed VdIIR and FdIIR VFD design methods explained at the beginning of Section 6.2 and listed on Tables 3-5 and 9. Using the same number of distinct variable coefficients at each of the four specified wideband cutoff frequencies, design results indicate that: (a) When compared to the corresponding FIR VFD filters (KJ; LD) shown in Table 6: As seen from Table 5, all the design methods (except (ZK)) for VdIIR and FdIIR VFD filters could achieve improved e_{rms} performances. (b) When compared to the corresponding AP VFD filters (KJ; LCR) shown in Table 6, the following VdIIR VFD filters could achieve improved e_{rms} performances: (i) (29) over (LCR) for α = 0.9625 (see Table 5); (ii) (35) over (KJ; LCR) for α = 0.9625 and over (LCR) for α = 0.95 (see Table 5); and (iii) (43) over (KJ; LCR) for $0.925 \le \alpha \le 0.9625$ (see Table 9). (c) When compared to the corresponding AP VFD filters (KJ; LCR) shown in Table 6, the following FdIIR VFD filters could achieve improved e_{rms} performances: (i) (29) over (LCR) for α = 0.9625 (see Table 5); (ii) (34) over (KJ; LCR) for α = 0.9625 and over (LCR) for α = 0.95

(see Table 5); (iii) (43) over (KJ; LCR) for $\alpha = 0.9625$ and over (LCR) for $\alpha = 0.95$ (see Table 9); (iv) (KJ) over (LCR) for $0.95 \leq \alpha \leq 0.9625$ (see Table 5); and (v) (TCK) over (LCR) for $\alpha = 0.9625$ (see Table 5).

Due to the mirror symmetric coefficient relation in an allpass VFD filter and for stability reason, it is a common practice to select its mean group delay to be the same as its filter order. Based on Table 10, as a decreases from 0.9625 to 0.9, the reductions in mean group delay values of (a) VdIIR VFD filters versus AP VFD filters range approximately from 1.5 to 1.6 times; and (b) FdIIR VFD filters versus AP VFD filters are higher and range approximately from 1.7 to 1.6 times.

The maximum pole radius versus fractional delay t of the four VdIIR VFD filters as listed in Table 9 and the four AP VFD filters designed by (KJ) and (LCR) are plotted with 1001 points, respectively, in Figs. 13-15. Figs. 13-15 indicate that all the three types of variable-denominator designs are stable; and the maximum pole radius at any t reduces as the passband cutoff frequency is lowered. As a general trend, it can be observed from the results that the error performances of each type of the VdIIR VFD filters, the FdIIR VFD filters, the AP VFD filters, and the FIR VFD filters improves along with a reduction in filter order with decreasing passband cutoff frequency $\alpha\pi$.

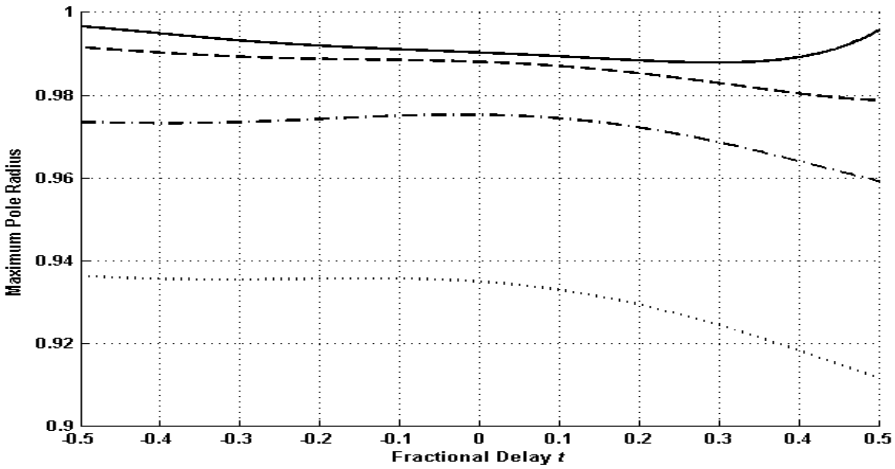

Fig. 13. Maximum pole radius of VdIIR VFD filter obtained by gradient-based design method with (43) versus fractional delay t (Solid: $a = 0.9625$, $N = 49$, $M = 6$, $D = 37$; Dashed: $a = 0.95$, $N = 46$, $M = 6$, $D = 35$; Dash-dot: $a = 0.925$, $N = 41$, $M = 6$, $D = 30$; Dotted: $a = 0.90$, $N = 36$, $M = 6$, $D = 27$)

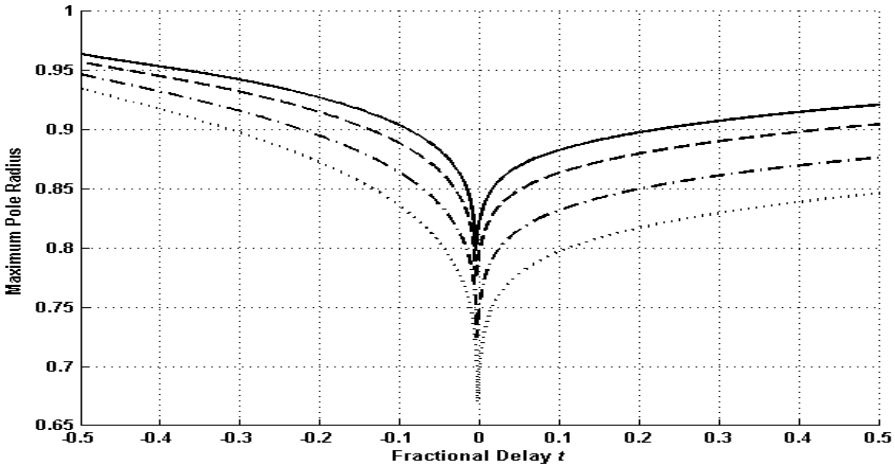

Fig. 14. Maximum pole radius of allpass VFD filter designed by (Kwan & Jiang, 2009a) versus fractional delay t (Solid: a = 0.9625, $M_{AP} = D_{AP}$ = 56; Dashed: a = 0.95, $M_{AP} = D_{AP}$ = 53; Dash-dot: a = 0.925, $M_{AP} = D_{AP}$ = 48; Dotted: a = 0.90, $M_{AP} = D_{AP}$ = 43)

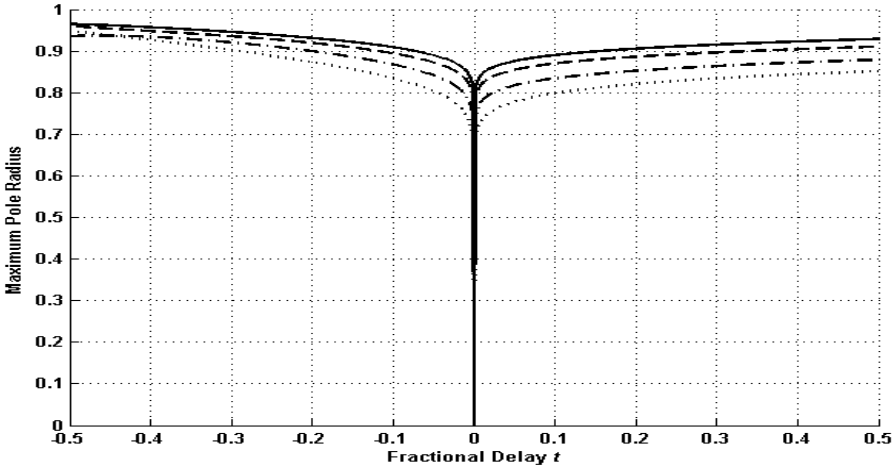

Fig. 15. Maximum pole radius of allpass VFD filter designed by (Lee et al., 2008) versus fractional delay t (Solid: a = 0.9625, $M_{AP} = D_{AP}$ = 56; Dashed: a = 0.95, $M_{AP} = D_{AP}$ = 53; Dash-dot: a = 0.925, $M_{AP} = D_{AP}$ = 48; Dotted: a = 0.90, $M_{AP} = D_{AP}$ = 43)

7. Summary

This chapter introduces an integrated design of IIR variable fractional delay (VFD) digital filters with variable and fixed denominators. Both sequential and gradient-based design approaches in the weighted least-squares (WLS) sense are adopted. The results obtained are compared to other design methods for IIR, allpass, and FIR VFD filters. In the sequential design method, the Levy's method is adopted along with an iterative reweighting technique

to transform the original nonconvex approximation error into a (convex) quadratic form. The design problem (at each iteration) can be further cast as a second-order cone programming (SOCP) problem. The stability of such a designed IIR VFD filter can be ensured by imposing a set of linear stability constraints derived from a sufficient condition in terms of the positive realness. In the gradient-based design method, a simple SOCP problem is first formulated using the Levy's method. The design is then refined through a local search starting from the initial design obtained. The stability of the initial filter can be ensured by the linear positive-realness based stability constraints or with the use of a regularization term aimed to suppress the energy of the denominator coefficients. Four sets of wideband filter examples are adopted with performances analyzed to illustrate the performances of the proposed design methods.

8. Conclusions

In this chapter, an integrated sequential design method and an integrated gradient-based design method for IIR VFD filters with variable-denominator and fixed-denominator have been presented. In contrast to the previous two-stage design methods, by merging the polynomial coefficient fitting into each respective integrated design, the approximation error caused by a separate polynomial coefficient fitting stage is eliminated. Also, instead of modeling denominator and optimizing numerator in separate steps, each of the sequential and gradient-based design methods jointly optimizes the numerator and denominator coefficients. Consequently, during the design procedure any change on any numerator or denominator coefficient can be utilized to optimize all the numerator and denominator coefficients in the subsequent design procedure. This facilitates the search of a better design in the coefficient vector space. The results of four sets of wideband filter examples designed using the proposed design methods, the VdIIR VFD (ZK) and the FdIIR VFD (KJ; TCK) design methods, and a number of AP VFD (KJ; LCR) and FIR VFD (KJ; LD) design methods indicate that IIR VFD filters could achieve some e_{rms} improvements over the other two types of VFD filters along with reduced mean group delays when compared to AP VFD filters. In particular, e_{rms} improvements can be observed in (a) the proposed gradient-based VdIIR design (with (43)) for wider band designs with $0.925 \le \alpha \le 0.9625$; and (b) the proposed gradient-based FdIIR design (with (43)) for the widest band design with $\alpha = 0.9625$. For narrower band designs such as $\alpha = 0.9$, e_{rms} improvements become obvious in the AP VFD designs (KJ; TCK). In term of design complexity, the FIR VFD designs (KJ; LD) remain to be the simplest. Finally, it should be emphasized that the error performances of a VFD filter design depend not only on the type (IIR, AP, and FIR) of VFD filters, but also depend on the effectiveness of its design method.

9. References

Brandenstein, H. & Unbehauen, R. (1998). Least-squares approximation of FIR by IIR digital filters. *IEEE Transactions on Signal Processing*, Vol. 46, No. 1, (January 1998), pp. 21-30, ISSN 1053-587X.

Brandenstein, H. & Unbehauen, R. (2001). Weighted least-squares approximation of FIR by IIR digital filters. *IEEE Transactions on Signal Processing*, Vol. 49, No. 3, (March 2001), pp. 558-568, ISSN 1053-587X.

Deng, T.-B. (2001). Discretization-free design of variable fractional-delay FIR filters. *IEEE Transactions on Circuits and Systems II*, Vol. 48, No. 6, (June 2001), pp. 637–644, ISSN 1057-7130.

Deng, T.-B. (2006). Noniterative WLS design of allpass variable fractional-delay digital filters. *IEEE Transactions on Circuits and Systems I*, Vol. 53, No. 2, (February 2006), pp. 358–371, ISSN 1549-8328.

Deng, T.-B. & Lian, Y. (2006). Weighted-least-squares design of variable fractional-delay FIR filters using coefficient symmetry. *IEEE Transactions on Signal Processing*, Vol. 54, No. 8, (August 2006), pp. 3023-3038, ISSN 1053-587X.

Dumitrescu, B. & Niemistö, R. (2004). Multistage IIR filter design using convex stability domains defined by positive realness. *IEEE Transactions on Signal Processing*, Vol. 52, No. 4, (April 2004), pp. 962-974, ISSN 1053-587X.

Jiang, A. & Kwan, H. K. (2009a). IIR digital filter design with novel stability criterion based on argument principle. *IEEE Transactions on Circuits and Systems I*, Vol. 56, No. 3, (March 2009), pp. 583-593, ISSN 1549-8328.

Jiang, A. & Kwan, H. K. (2009b). Iterative design of IIR variable fractional delay digital filters, *Proceedings IEEE International Conference on Electro/Information Technology*, pp. 163–166, Print ISBN 978-1-4244-3354-4, Windsor, ON, Canada, June 7–9, 2009.

Kwan, H. K., Jiang, A., & Zhao, H. (2006). IIR variable fractional delay digital filter design, *Proceedings of TENCON*, PO5.27, TEN-863, pp. 1-4, ISBN 1-4244-0549-1/Print ISBN 1-4244-0548-3, Hong Kong, November 14-17, 2006.

Kwan, H. K. & Jiang, A. (2007). Design of IIR variable fractional delay digital filters, *Proceedings of IEEE International Symposium on Circuits and Systems*, pp. 2714-2717, Print ISBN 1-4244-0920-9, New Orleans, May 27-30, 2007.

Kwan, H. K. & Jiang, A. (2009a). FIR, allpass, and IIR variable fractional delay digital filter design. *IEEE Transactions on Circuits and Systems I,* Vol. 56, No. 9, (September 2009), pp. 2064-2074, ISSN 1549-8328.

Kwan, H. K. & Jiang, A. (2009b). Low-order fixed denominator IIR VFD filter design, *Proceedings of IEEE International Symposium on Circuits and Systems*, pp. 481-484, Print ISBN 978-1-4244-3827-3, Taipei, Taiwan, May 24-27, 2009.

Laakso, T. I., Valimaki, V., Karjalainen, M., & Laine, U. K. (1996). Splitting the unit delay. *IEEE Signal Processing Magazine*, Vol. 13, No. 1, (January 1996), pp. 30-60, ISSN 1053-5888.

Lee, W. R., Caccetta, L., & Rehbock, V. (2008). Optimal design of all-pass variable fractional-delay digital filters. *IEEE Transactions on Circuits and Systems I*, Vol. 55, No. 5, (June 2008), pp. 1248–1256, ISSN 1549-8328.

Levy, E. C. (1959). Complex curve fitting. *IRE Transactions on Automatic Control*, Vol. AC-4, (May 1959), pp. 37-43, ISSN 0096-199X.

Lu, W.-S., Pei, S.-C., & Tseng, C.-C. (1998). A weighted least-squares method for the design of stable 1-D and 2-D IIR digital filters. *IEEE Transactions on Signal Processing*, Vol. 46, No. 1, (January 1998), pp. 1–10, ISSN 1053-587X.

Lu, W.-S. & Deng, T.-B. (1999). An improved weighted least-squares design for variable fractional delay FIR filters. *IEEE Transactions on Circuits and Systems II,* Vol. 46, No. 8, (August 1999), pp. 1035–1040, ISSN 1057-7130.

Lu, W.-S. (1999). Design of stable IIR digital filters with equiripple passbands and peak-constrained least-squares stopbands. *IEEE Transactions on Circuits and Systems II*, Vol. 46, No. 11, (November 1999), pp. 1421-1426, ISSN 1057-7130.

Sanathanan, C. K. & Koerner, J. (1963). Transfer function synthesis as a ratio of two complex polynomials. *IEEE Transactions on Automatic Control*, Vol. AC-8, No. 1, (January 1963), pp. 56-58, ISSN 0018-9286.

Sturm, J. F. (1999). Using SeDuMi 1.02, a MATLAB toolbox for optimization over symmetric cones. *Optimization Methods and Software,* Vol. 11-12, 1999, pp. 625-653, Print ISSN 1055-6788/Online ISSN 1029-4937.

Tseng, C.-C. & Lee, S.-L. (2002). Minimax design of stable IIR digital filter with prescribed magnitude and phase responses. *IEEE Transactions on Circuits and Systems I*, Vol. 49, No. 4, (April 2002), pp. 547-551, ISSN 1549-8328.

Tseng, C.-C. (2002a). Eigenfilter approach for the design of variable fractional delay FIR and all-pass filters. *IEE Proceedings - Visual, Image, Signal Processing*, Vol. 149, No. 5, (October 2002), pp. 297-303, ISSN 1350-245X.

Tseng, C.-C. (2002b). Design of 1-D and 2-D variable fractional delay allpass filters using weighted least-squares method. *IEEE Transactions on Circuits and Systems I*, Vol. 49, No. 10, (October 2002), pp. 1413–1422, ISSN 1549-8328.

Tseng, C.-C. (2004). Design of stable IIR digital filter based on least *p*-power error criterion. *IEEE Transactions on Circuits and Systems I*, Vol. 51, No. 9, (September 2004), pp. 1879-1888, ISSN 1549-8328.

Tsui, K. M., Chan, S. C., & Kwan, H. K. (2007). A new method for designing causal stable IIR variable fractional delay digital filters. *IEEE Transactions on Circuits and Systems II*, Vol. 54, No. 11, (November 2007), pp. 999–1003, ISSN 1057-7130.

Zhao, H. & Kwan, H. K. (2005). Design of 1-D stable variable fractional delay IIR filters, *Proceedings of International Symposium on Intelligent Signal Processing and Communication Systems*, pp. 517-520, ISBN 978-0-7803-9266-3, Hong Kong, December 13-16, 2005.

Zhao, H. & Yu, J. (2006). A simple and efficient design of variable fractional delay FIR filters. *IEEE Transactions on Circuits and Systems II,* Vol. 53, No. 2, (February 2006), pp. 157–160, ISSN 1057-7130.

Zhao, H., Kwan, H. K., Wan, L., & Nie, L. (2006). Design of 1-D stable variable fractional delay IIR filters using finite impulse response fitting, *Proceedings of International Conference on Communications, Circuits and Systems*, pp. 201-205, ISBN 978-0-7803-9584-8, Guilin, China, June 25-28, 2006.

Zhao, H. & Kwan, H. K. (2007). Design of 1-D stable variable fractional delay IIR filters. *IEEE Transactions on Circuits and Systems II*, Vol. 54, No. 1, (January 2007), pp. 86–90, ISSN 1057-7130.

Digital Filters

Edited by Prof. Fausto Pedro GarcÃa MÃ¡rquez

ISBN 978-953-307-190-9
Hard cover, 290 pages
Publisher InTech
Published online 11, April, 2011
Published in print edition April, 2011

The new technology advances provide that a great number of system signals can be easily measured with a low cost. The main problem is that usually only a fraction of the signal is useful for different purposes, for example maintenance, DVD-recorders, computers, electric/electronic circuits, econometric, optimization, etc. Digital filters are the most versatile, practical and effective methods for extracting the information necessary from the signal. They can be dynamic, so they can be automatically or manually adjusted to the external and internal conditions. Presented in this book are the most advanced digital filters including different case studies and the most relevant literature.

How to reference

In order to correctly reference this scholarly work, feel free to copy and paste the following:

Hon Keung Kwan and Aimin Jiang (2011). Integrated Design of IIR Variable Fractional Delay Digital Filters with Variable and Fixed Denominators, Digital Filters, Prof. Fausto Pedro GarcÃa MÃ¡rquez (Ed.), ISBN: 978-953-307-190-9, InTech, Available from: http://www.intechopen.com/books/digital-filters/integrated-design-of-iir-variable-fractional-delay-digital-filters-with-variable-and-fixed-denominat

INTECH
open science | open minds

InTech Europe
University Campus STeP Ri
Slavka Krautzeka 83/A
51000 Rijeka, Croatia
Phone: +385 (51) 770 447
Fax: +385 (51) 686 166
www.intechopen.com

InTech China
Unit 405, Office Block, Hotel Equatorial Shanghai
No.65, Yan An Road (West), Shanghai, 200040, China
中国上海市延安西路65号上海国际贵都大饭店办公楼405单元
Phone: +86-21-62489820
Fax: +86-21-62489821